Deformation of the zygomaticomaxillary and nasofrontal sutures during bone-anchored maxillary protraction and reverse-pull headgear treatments: An ex-vivo study

Ayman Al Dayeh, Richard A. Williams, Terry M. Trojan, and Wanda I. Claro
Memphis, Tenn

Introduction: Bone-anchored maxillary protraction (BAMP) is an emerging treatment that involves applying a protraction load to the maxillary bone. Although it is believed that such an approach results in better sutural separation, this has not been investigated. This study aimed to assess and compare the deformation of 1 circumaxillary suture (zygomaticomaxillary suture [ZMS]) and 1 facial suture (nasofrontal suture [NFS]) during BAMP and reverse-pull headgear (RPHG) treatment. **Methods:** The study was performed ex vivo on 15 pig heads. Miniplates were placed in the maxillary bone and the body of the mandible. A molar tube was bonded to the maxillary first molars. Six single-element strain gauges and 3 differential variable reluctance transducers were installed across the ZMS and NFS bilaterally. Each head underwent BAMP and RPHG unilaterally and bilaterally. **Results:** In unilateral experiments, both BAMP and RPHG resulted in tension on the ipsilateral ZMS and NFS and compression on the contralateral side, with higher magnitude in the BAMP group. In bilateral experiments, both modalities resulted in tension at the ZMS, with higher magnitude in the BAMP group. Deformation of the NFS was different between the 2 groups: tension in majority of the BAMP and compression in most of the RPHG heads. **Conclusions:** Our study shows a higher magnitude of sutural separation in BAMP than in RPHG. The pattern of sutural deformation is consistent with a forward displacement of the midface in BAMP compared with an upward and backward rotation in the RPHG. Rotation of the maxilla was also present in some of the subjects who underwent BAMP. (Am J Orthod Dentofacial Orthop 2019;156:745-57)

Class III is certainly not a rare malocclusion with an average global prevalence of approximatelty 7%.[1] Most patients with Class III malocclusion are characterized by various combinations of maxillary deficiency and mandibular excess.[2] Generally, 3 treatment options exist for such patients, including orthopedic intervention in growing patients, dental camouflage, and orthognathic surgery. The orthopedic intervention is the treatment of choice because it corrects the underlying skeletal discrepancy without the esthetic compromises associated with dental camouflage, and the morbidity and expenses associated with orthognathic surgeries.

Reverse-pull head gear (RPHG) had been the traditional orthopedic treatment of choice for patients with Class III malocclusion exhibiting maxillary deficiency.[3] With this approach, the protraction force is applied to the maxilla using maxillary teeth as a point of the force application. RPHG results in separation of circummaxillary sutures and stimulation of bone formation along the sutural edges.[4,5] However, as RPHG load is applied through the dentition, most of the loading force is dissipated across the teeth, which results in unwanted dental side effects such as excessive proclination of maxillary teeth and downward and backward rotation

From the Department of Orthodontics, College of Dentistry, University of Tennessee Health Science Center, Memphis, Tenn.
All authors have completed and submitted the ICMJE Form for Disclosure of Potential Conflicts of Interest, and none were reported.
This project was supported by the American Association of Orthodontists Foundation Orhan C. Tuncay and T.M Graber Teaching Fellowship Awards (2015, 2017).
Address correspondence to: Ayman Al Dayeh, Department of Orthodontics, Room S301, 875 Union Ave, Memphis, TN 38163; e-mail, aaldayeh@uthsc.edu.
Submitted, May 2018; revised and accepted, December 2018.
0889-5406/$36.00

https://doi.org/10.1016/j.ajodo.2018.12.019

of the mandible.[6,7] It is believed that <50% of the correction achieved in RPHG is because of true skeletal changes. An additional limitation associated with the use of RPHG is that its potential for orthopedic correction greatly diminishes with age, probably because of increased sutural digitation.[8] It is recommended to start RPHG treatment in the mixed dentition.[9]

Several authors have recommended applying the protraction force directly to the maxillary bone to achieve better sutural loading. In a pioneering study, Kokich et al[10] reported the successful application of protraction directly to the maxilla in a patient with Class III malocclusion, using ankylosed primary canines. Smalley et al[11] reported that applying RPHG to titanium implants placed in the maxilla and the zygomatic bone in monkeys resulted in a greater separation of the zygomaticomaxillary (ZMS) and zygomaticotemporal (ZTS) sutures. With the advent of temporary skeletal anchorage devices, several studies have reported on applying RPHG load to temporary skeletal anchorage devices in the nasal area and the malar bone.[12-16] Most of these studies suggested that applying the protraction load directly to the maxilla resulted in a better outcome compared with the outcome observed in traditional tooth-supported RPHG. This improved outcome is generally attributed to increased loading of the sutures.

Another limitation associated with RPHG is the unesthetic appearance of the extraoral portion of the device, resulting in poor patient compliance and a compromised outcome. To address this, De Clerck[17] introduced the concept of the intraoral bone-anchored maxillary protraction (BAMP). It consists of surgical placement of miniplates in the maxillary bone anterior to the ZMS and the body of the mandible in the canine area. Patients then apply intermaxillary elastics between the 2 plates. Applying a protraction load directly to the maxilla resulted in more protraction.[18] The intraoral protraction system is believed to result in better patient compliance. In a series of studies, it was reported that BAMP resulted in more protraction of the maxilla and zygoma, more significant improvement in the anteroposterior position of the maxilla, and favorable rotation of the mandible.[17-23]

Although several studies have examined the clinical effects of BAMP, its effects on sutural loading and bone formation are still poorly understood. Ito et al[24] were the first to report the BAMP effects on sutures. Using 3-month-old dogs, they reported that BAMP resulted in a 7-fold increase in bone apposition at the ZMS compared with untreated controls. In a pilot study,[25] BAMP resulted in nearly a 2-fold increase in bone apposition and an increase in osteocalcin expression at the ZMS compared with controls. However, both studies did not compare BAMP with RPHG, which is the current treatment of choice for patients with maxillary hypoplasia. BAMP is associated with higher treatment cost and 2 additional minor surgeries. Thus, improving the predictability and optimizing the treatment outcome is essential.

Sutural loading is known to stimulate bone formation at the sutural edges.[26] The relationship between magnitude, pattern, and duration of the load to subsequent bone formation is still an ongoing controversy. Although some authors reported that higher constant tension resulted in more bone formation,[27,28] others have reported that an oscillatory load is more efficient.[29,30] Understanding the effects of such variables in the context of BAMP and RPHG will help clarify whether the improved outcome in BAMP is because of improved sutural loading. In addition, such understanding will lead to a BAMP loading protocol that is less anecdotal than the current protocol.[17]

The observed difference in mandibular rotation between RPHG and BAMP is clear. One of the side effects of RPHG is a downward and backward rotation of the mandible, resulting in increased vertical dimension and poor profile appearance, especially in patients with hyperdivergent facial phenotype.[3,7,18,31] Preliminary clinical findings from BAMP studies suggest a more anterior bodily movement of the maxilla and posterior movement of the condyle while controlling mandibular rotation.[20,32]

To date, scarce information exists on the deformation of the circumaxillary sutures during BAMP. In addition, the difference in sutural loading between BAMP and RPHG has never been investigated. Determining how BAMP loads facial sutures will help clinicians understand and optimize the treatment. Comparing sutural deformation during RPHG and BAMP may help to explain some of the differences in the clinical outcomes between the 2 groups. This study aimed to measure the deformation of the ZMS and nasofrontal sutures (NFS) during BAMP and RPHG, focusing on the difference in magnitude and direction of sutural loading between the 2 groups. Two types of sensors were used to assess sutural deformation, including strain gauges and linear displacement sensors. The high sensitivity and resolution of those sensors allow measuring aspects of sutural deformation that cannot be detected using standard clinical tools such as cone-beam computed tomography scans. The ZMS is 1 of the circummaxillary sutural systems and was chosen because it is considered the principal target of maxillary protraction therapy.[4,33] Deformation of the NFS was assessed because its dorsal location, relative to the ZMS, will help determine the overall pattern of midfacial deformation during protraction. In addition, because the NFS is not

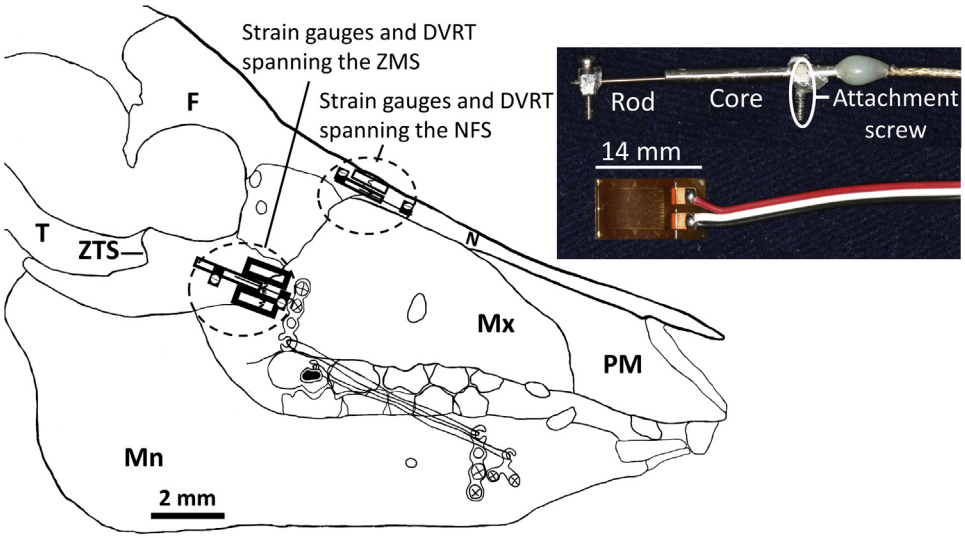

Fig 1. Lateral drawing of a pig skull illustrating the location of the miniplates and sensors. *Top*, Picture of a DVRT illustrating different parts of the sensor. *Bottom*, Strain gauge. *F*, frontal bone; *N*, nasal bone; *PM*, premaxillary bone; *Mx*, maxillary bone; *Mn*, mandible; *T*, temporal bone.

directly attached to the maxilla, measuring its deformation will help understand how protraction loads affect sutures that are not directly attached to the maxilla. The null hypothesis is that there is no difference in the magnitude of ZMS separation between BAMP and RPHG.

MATERIALS AND METHODS

The study was performed ex vivo on pig heads. Fifteen pig heads were obtained from a local abattoir. Age and breed were unknown, but all animals were in the late mixed or early permanent dentition. After killing these animals, their heads were stored at approximately 2°C by the abattoir. Heads were acquired 1-4 days postmortem and were stored frozen at −20°C until the day of the experiment. Heads were left to thaw at room temperature for 12 hours before each experiment. Both BAMP and RPHG were performed on the same heads. BAMP was performed first, followed by RPHG on the first 8 consecutive heads, while RPHG was performed first on the remaining 7 consecutive heads. The following procedure was performed on all heads (Fig 1). The zygomatic process of the maxillary bone and the body of the mandible were exposed. Two miniplates were fixed to the right and left maxillary bone approximately 5 mm anterior to the ZMS using 2 × 12-mm miniscrews. Two miniplates were fixed to the body of the mandible anterior to the first premolar using 2-3 × 10-mm miniscrews. The distance between the miniplates was adjusted, so the intermaxillary elastics yielded a 200 gram-force (gf), verified by a force gauge. The direction of the protraction force was 25° ± 4° to the occlusal plane. The load was applied from a molar tube to a miniplate placed in the mandible to mimic the RPHG. The buccal surfaces of the maxillary first molars were etched and primed using Transbond Self-Etching Primer (3M Unitek, Monrovia, Calif) followed by AssurePlus (Reliance Inc, Itasca, Ill). A molar tube was bonded using transbond adhesive (3M Unitek). A second mandibular miniplate was fixed as before. The location of the second mandibular miniplate was adjusted, so the generated RPHG protraction force was 200 gf per elastic with a similar angle to the occlusal plane as with BAMP.

The surfaces of the ZMS and NFS were exposed, cauterized, and dehydrated. Two single element strain gauges (Vishay Micro-Measurements, Raleigh, NC) were bonded across the superior and inferior parts of the ZMS using cyanoacrylate. A third gauge was bonded across the NFS. The procedure was repeated on the contralateral side. Teflon tape was placed on the suture before gluing to maintain the sutural patency. Three differential variable reluctance transducers (DVRTs; LORD Microstrain Inc, Williston, Vt) were installed across the right and left ZMS and the NFS. DVRT wires were connected to a signal demodulator (DEMOD-DC2, LORD Microstrain Inc) and together with the strain gauges (SGs) were connected to a wireless transmitter (V-link, LORD Microstrain Inc). SGs and DVRT signals were streamed to a nearby computer with a Universal Serial

Bus base station, operating NodeCommander software (LORD Microstrain Inc). These 2 types of sensors recorded 2 aspects of sutural deformation, including strain (strain gauge; values in με) and linear separation (DVRT; values in μm).

Each head was loaded using both BAMP and RPHG. For each of the 2 treatment modalities, heads were loaded unilaterally and bilaterally, and the deformation of the sutures was measured by the SGs and DVRTs. Unilateral loading consisted of adding 5 consecutive elastics, 200 gf each. Forces were then removed. The procedure was then repeated on the contralateral side. Bilateral loading was performed by progressively adding 200 gf on the right followed by 200 gf on the left side until 1000 gf per side was reached. Although the 1000 gf was still in place, the mandible was then moved to the right and left to verify the functionality of the sensors, followed by holding the snout bilaterally and applying forward force to the mandible for approximately10 seconds. Throughout the experiment, the attachment of the mandible to the maxilla was maintained. Because of the increased stiffness of the muscles of mastication postmortem, the extent of mandibular movements was limited.

Forces were then removed from the right side, followed by the left side. Sensors were removed and inspected for damage. The streamed files were recorded as Comma Separated Value format (*.csv) by NodeCommander. Files were then converted to a text file (*.txt) and opened and analyzed in AcqKnowledge software (Biopac, Calif). Data were summarized using Excel (Microsoft, Redmond, Wash). For the strain gauges, sutural deformation was calculated per 200 gf in the unilateral experiments and after each pair of the 200 gf were applied on the right and left side in the bilateral experiments. For the DVRTs, sutural elongation was measured after the entire 1000 gf (5 elastics were applied).

Statistical analysis

Because of the small sample size and variability, data were analyzed using the nonparametric Wilcoxon signed rank test with SPSS software (v. 25, IBM, Armonk, NY).

RESULTS

The magnitude of sutural deformation increased with increased force magnitude in both the BAMP and RPHG groups. However, this increase was not always equal or linear. As a result, the strain gauge data were reported as an average of the deformations recorded after each of the 200 gf elastics were applied in the unilateral protraction; and as an average of the deformations after each pair of the 200 gf elastics was applied in the bilateral protraction. There was a great overlap between the DVRT and SG data. Consequently, a descriptive summary of the DVRT data is reported only for the bilateral part of the study to avoid the introduction of redundant and possibly confusing information.

Figure 2 illustrates a typical Acqknowledge recording of the unilateral BAMP experiments. No significant difference was found between the right and left ipsilateral deformations or between the right and left contralateral deformations in both the BAMP and RPHG groups ($P > 0.1$). As a result, the right and left side values were averaged for the ipsilateral and contralateral locations (Table I; Fig 3).

In the unilateral BAMP group, no difference was found between the deformation at the superior and inferior ZMS within the ipsilateral and contralateral sites. Deformation at the NFS in the contralateral group was significantly lower (more compression) than deformation at the ZMS in the same group ($P = 0.03$). Deformation at the NFS in the ipsilateral group was lower (less tension) than deformation at the ZMS; however, it did not reach statistical significance ($P = 0.06$).

In the unilateral RPHG group, no difference was found between the deformation at the superior and inferior ZMS within the ipsilateral and contralateral groups. Deformation at the NFS was significantly lower than deformation at the corresponding ipsilateral (less tension) and contralateral (more compression) ZMS ($P < 0.02$).

Although the magnitude of strain was generally higher in the BAMP group (more tension in the ipsilateral and more compression in the contralateral) than in the RPHG group, it did not reach statistical significance at any of the sites ($P > 0.08$).

Figure 4 illustrates a typical Acqknowledge recording of bilateral BAMP experiments. The wave pattern in the bilateral experiments was characterized by an alternating higher tension (when ipsilateral force was installed) and low compression (when contralateral force was placed); the net result was tension. Values from the bilateral protraction are reported in Tables II-IV and Figures 5 and 6.

Overall, all the ZMS sites in the BAMP group displayed tension with great individual variability. The deformation at the NFS was not uniform: although most animals displayed tension at the NFS, compression was noticed in some animals. Higher deformation (more tension) was found at the inferior compared with superior ZMS on the right and left sides ($P < 0.04$). Although the tension at the superior ZMS was higher than tension at the NFS, this difference

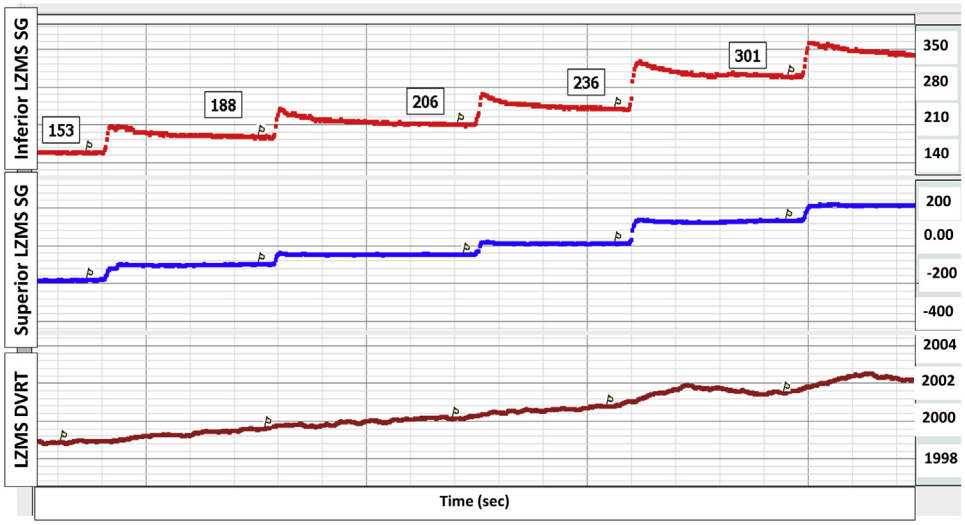

Fig 2. Recording of the deformation of the inferior and superior LZMS during ipsilateral protraction as recorded by the strain gauges and DVRT. Flags correspond to new elastic (200 gf) placement. Numbers correspond to the deformation reading for each sensor. An incremental increase in force application resulted in increased tension at the suture.

Table I. Deformation of the ipsilateral and contralateral ZMS and NFS during unilateral protraction recorded by the SGs

	Ipsilateral side (side of force application)						*Contralateral side*					
	Inferior ZMS		*Superior ZMS*		*NFS*		*Inferior ZMS*		*Superior ZMS*		*NFS*	
Pig number	*BAMP*	*RPHG*	*BAMP*	*RPHG*	*BAMP*	*RPHG*	*BAMP*	*RPHG*	*BAMP*	*RPHG*	*BAMP*	*RPHG*
53	25 ± 20	5 ± 2	12 ± 8	8 ± 7	13 ± 2	3 ± 0	−4 ± 3	−3 ± 2	−5 ± 1	−3 ± 1	−8 ± 0	−16 ± 7
54	27 ± 19	26 ± 20	33 ± 21	34 ± 1	20 ± 1	12 ± 1	−3 ± 6	−29 ± 24	−6 ± 13	−19 ± 18	−8 ± 1	−29 ± 3
55	79 ± 25	52 ± 18	79 ± 4	67 ± 14	35 ± 26	34 ± 8	−31 ± 0	−9 ± 2	−45 ± 9	−30 ± 12	−76 ± 25	−34 ± 8
56	29 ± 26	23 ± 17	24 ± 20	17 ± 6	0 ± 25	3 ± 11	−19 ± 11	−15 ± 2	−11 ± 9	−10 ± 1	−35 ± 10	−51 ± 30
57	37 ± 3	9 ± 3	29 ± 17	9 ± 8	17 ± 4	0 ± 3	−13 ± 16	−6 ± 4	−19 ± 3	−6 ± 5	1 ± 1	−5 ± 3
58	22 ± 2	32 ± 14	31 ± 22	37 ± 21	22 ± 8	19 ± 15	−11 ± 7	−9 ± 7	−12 ± 13	−12 ± 7	1 ± 3	−33 ± 7
59	28 ± 19	20 ± 1	28 ± 31	19 ± 4	0 ± 41	11 ± 3	−11 ± 1	−10 ± 11	−10 ± 10	−11 ± 2	−24 ± 22	−21 ± 2
60*	NA	NA	NA	NA	NA	NA	NA	NA	NA	NA	NA	NA
61	18 ± 49	68 ± 34	29 ± 47	54 ± 15	−4 ± 4	6 ± 8	−28 ± 42	−9 ± 2	−1 ± 54	−14 ± 17	−2 ± 13	−6 ± 15
62	42 ± 14	24 ± 17	36 ± 8	25 ± 17	38 ± 22	19 ± 10	−21 ± 10	−17 ± 4	−17 ± 11	−15 ± 10	−33 ± 16	−30 ± 10
63	54 ± 22	38 ± 20	39 ± 6	49 ± 29	19 ± 13	14 ± 28	−13 ± 34	−22 ± 28	−31 ± 28	−14 ± 12	−51 ± 10	−28 ± 11
64	12 ± 8	7 ± 8	29 ± 11	17 ± 10	4 ± 13	17 ± 2	−6 ± 9	−7 ± 6	−4 ± 2	−5 ± 2	−28 ± 7	−6 ± 9
65	6 ± 1	8 ± 3	24 ± 3	5 ± 3	44 ± 18	10 ± 1	−2 ± 1	−6 ± 4	−8 ± 1	−6 ± 3	7 ± 4	−3 ± 1
66	21 ± 5	21 ± 5	45 ± 23	28 ± 26	39 ± 57	44 ± 4	−23 ± 6	−16 ± 14	−6 ± 1	−7 ± 15	−56 ± 17	−76 ± 8
67	22 ± 28	5 ± 4	5 ± 3	2 ± 2	23 ± 3	−1 ± 3	−6 ± 3	−3 ± 1	−6 ± 3	−2 ± 1	−17 ± 13	−14 ± 2
Mean ± SD	30 ± 19	24 ± 19	32 ± 17	27 ± 20	19 ± 16	14 ± 13	−14 ± 9	−12 ± 7	−13 ± 12	−11 ± 7	−24 ± 25	−25 ± 20
Median	26	22	29	22	20	12	−12	−9	−9	−11	−21	−25

The values are the average of the right and left sides and are reported per 200 gf. Values are in με. Negative numbers indicate compression.
NA, Not available; *SD*, standard deviation.
*No unilateral data recorded in pig number 60 because of error in file saving.

reached statistical significance only on the left side ($P = 0.05$; Table II; Fig 5). Higher linear deformation was recorded by the ZMS compared with the NFS DVRTs (Fig 6).

The RPHG displayed a different pattern of deformation compared with the BAMP. Although tension was noticed at the ZMS, the NFS were under compression in most of the examined sites (>90%). In the remaining

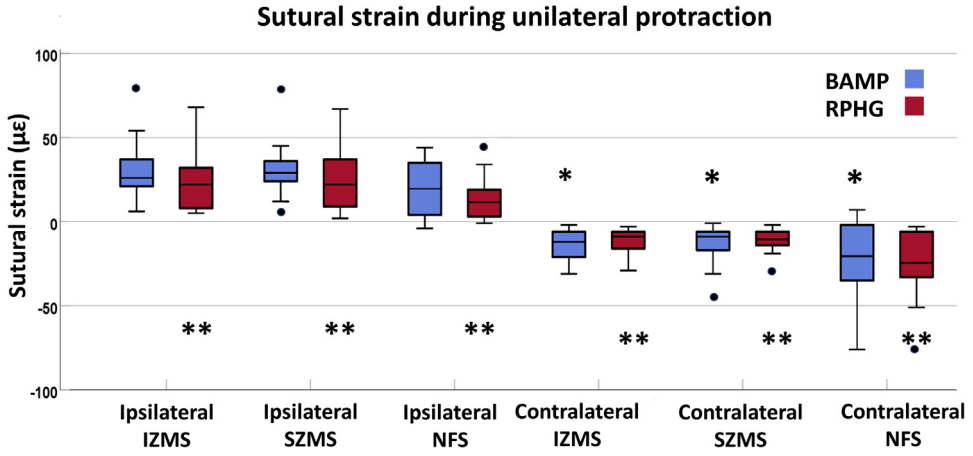

Fig 3. Box plot of the strain (per 200 gf) at the ipsilateral and contralateral ZMS and NFS recorded by the strain gauges during the unilateral protraction experiments. The medians are represented as the *solid black horizontal lines*. The *box boundaries* correspond to the 25th and 75th percentile. *Whiskers* cover the 5th and the 95th percentile. *Black dots* correspond to the outliers. *IZMS*, inferior zygomatico-maxillary suture; *SZMS*, superior zygomatico-maxillary suture. Signifcant differences: **P* <0.03 (within BAMP group); ***P* <0.02 (within RPHG group).

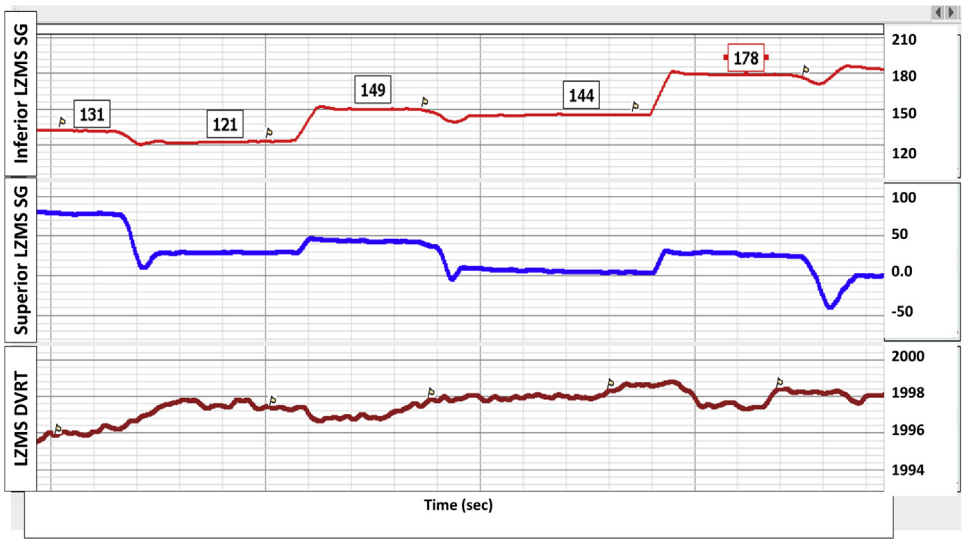

Fig 4. Deformation of the inferior and superior LZMS during bilateral protraction as recorded by the strain gauges and DVRT. Flags correspond to new added elastic (200 gf). In bilateral protraction, placing a force on the contralateral side resulted in compression, whereas placing the ipsilateral force resulted in tension. The net result of the 2 forces was mostly tension at the ZMS. Numbers correspond to the deformation reading for each sensor. Additional bilateral force placement resulted in a net increase in tension at the suture.

10 % (4 sites), 3 showed very minimal deformation, and 1 displayed tension. The tension seemed to decrease (moved dorsally) as evidenced by higher tension at the inferior ZMS followed by the superior ZMS and NFS (P <0.002; Table II; Fig 5). Similarly, higher linear deformation (tension) was present on the ZMS compared with the NFS DVRTs (Fig 6).

A comparison of the BAMP with RPHG showed consistently higher tension in the inferior and the superior ZMS in the BAMP group (P <0.01). Deformation at

Table II. Deformation of the RZMS, LZMS, RNFS, and LNFS recorded by the SGs

	Inferior RZMS		*Inferior LZMS*		*Superior RZMS*		*Superior LZMS*		*Right NFS*		*Left NFS*	
Pig number	*BAMP*	*RPHG*	*BAMP*	*RPHG*	*BAMP*	*RPHG*	*BAMP*	*RPHG*	*BAMP*	*RPHG*	*BAMP*	*RPHG*
53	44 ± 4	3 ± 1	12 ± 4	8 ± 7	4 ± 4	1 ± 1	4 ± 3	−1 ± 4	2 ± 3	−16 ± 9	1 ± 2	−17 ± 5
54*	NA	NA	NA	NA	NA	NA	NA	NA	NA	NA	NA	NA
55	62 ± 25	49 ± 12	38 ± 14	19 ± 19	29 ± 10	15 ± 17	47 ± 28	32 ± 14	−32 ± 26	−67 ± 52	−14 ± 18	−44 ± 6
56	47 ± 19	38 ± 16	23 ± 4	19 ± 10	10 ± 6	−1 ± 11	8 ± 3	12 ± 15	−8 ± 26	−118 ± 92	−32 ± 42	−126 ± 76
57	32 ± 11	19 ± 7	NA	NA	32 ± 5	16 ± 4	8 ± 7	−11 ± 6	21 ± 9	0 ± 2	23 ± 4	−6 ± 3
58	47 ± 26	10 ± 11	41 ± 12	43 ± 19	22 ± 16	8 ± 10	18 ± 23	12 ± 11	−20 ± 20	−46 ± 28	7 ± 24	−24 ± 20
59	31 ± 15	19 ± 20	29 ± 2	19 ± 9	10 ± 1	8 ± 6	5 ± 5	6 ± 13	14 ± 20	−27 ± 18	8 ± 10	−28 ± 21
60	NA	NA	31 ± 6	33 ± 21	63 ± 11	−37 ± 40	41 ± 6	33 ± 8	40 ± 5	−49 ± 55	21 ± 6	34 ± 31
61	41 ± 26	9 ± 9	64 ± 12	37 ± 20	73 ± 16	25 ± 8	65 ± 26	59 ± 25	−4 ± 4	−60 ± 24	3 ± 4	−39 ± 32
62	26 ± 20	20 ± 32	41 ± 8	26 ± 28	27 ± 14	3 ± 10	31 ± 5	23 ± 5	14 ± 10	−41 ± 52	−18 ± 30	0 ± 21
63	39 ± 11	51 ± 25	37 ± 14	39 ± 15	33 ± 8	−14 ± 30	22 ± 19	33 ± 33	10 ± 8	−39 ± 19	−39 ± 21	−70 ± 28
64	12 ± 9	1 ± 2	27 ± 20	17 ± 19	6 ± 5	4 ± 15	18 ± 12	16 ± 29	39 ± 34	−7 ± 15	41 ± 14	−4 ± 10
65	NA	NA	13 ± 3	12 ± 10	25 ± 5	7 ± 7	13 ± 3	−5 ± 2	41 ± 7	−1 ± 5	NA	NA
66	29 ± 25	30 ± 22	35 ± 16	26 ± 19	32 ± 22	1 ± 9	11 ± 8	10 ± 16	4 ± 108	−37 ± 69	−35 ± 54	−91 ± 46
67	39 ± 14	4 ± 2	7 ± 4	2 ± 1	3 ± 1	1 ± 1	−2 ± 3	−3 ± 27	44 ± 56	−16 ± 6	12 ± 5	−18 ± 3
Mean ± SD	37 ± 13†	21 ± 18†	31 ± 15†	23 ± 12†	26 ± 21†	3 ± 15†	21 ± 19	15 ± 19	9 ± 22	−37 ± 31	−2 ± 25	−33 ± 42
Median	39	19	31	19	26	4	14	12	7	−38	3	−24

The values are the average of the right and left sides and are reported per 200 gf. Values are in με. Negative numbers indicate compression.
NA, Not available; *SD*, standard deviation.
*No bilateral data from pig number 54 because of error in file saving; †Values were significantly higher in the BAMP than in RPHG.

Table III. Change in sutural deformation after the mandible was moved forward

	Inferior RZMS		*Inferior LZMS*		*Superior RZMS*		*Superior LZMS*		*Right NFS*		*Left NFS*	
Pig number	*BAMP*	*RPHG*	*BAMP*	*RPHG*	*BAMP*	*RPHG*	*BAMP*	*RPHG*	*BAMP*	*RPHG*	*BAMP*	*RPHG*
53	5	4	17	10	−6	−4	25	25	−65	37	−79	24
54*	NA	NA	NA	NA	NA	NA	NA	NA	NA	NA	NA	NA
56	6	−3	6	4	1	−2	4	−4	49	−83	55	−40
57	6	9	14	10	7	3	1	12	6	−6	16	29
58	10	15	25	3	23	9	−6	−3	79	36	80	32
59	6	8	11	15	17	8	5	−5	−18	0	44	0
61	14	115	20	72	50	−117	38	−177	−84	−14	−26	−105
62	9	12	10	11	3	7	−6	−6	11	−12	−10	−34
63	18	6	20	11	53	21	60	33	36	21	−113	−74
64	16	10	−15	−37	−41	26	−43	−31	−31	−256	−58	51
65	NA	NA	29	8	6	−20	65	−66	65	20	NA	NA
66	39	39	18	1	32	35	−47	40	74	160	−218	169
67	32	−4	30	0	12	0	47	2	211	81	−129	18
Mean ± SD	15 ± 11	19 ± 33	15 ± 12	9 ± 24	13 ± 25	−3 ± 39	12 ± 36	−15 ± 58	28 ± 78	−1 ± 99	−40 ± 90	6 ± 73
Median	10	9	18	9	10	5	5	−4	23	10	−26	18

Only strain gauges data are reported. Values are in με. Negative numbers indicate compression. Only animals with paired data from both BAMP and RPHG are reported.
NA, Not available; *SD*, standard deviation.
*No data from pig number 54 because of error in file saving.

the NFS was tensile in BAMP and compressive in RPHG ($P < 0.001$; Table II; Fig 5). Higher sutural separation (recorded by the DVRTs) was present in the BAMP group at the NFS and left zygomatico-maxillary suture (LZMS) sites (Fig 6).

Moving the mandible forward resulted in increased tension at the sites examined (Table III). Because of the high variability between various animals, values were reported, but no statistical analysis was performed.

Removing the protraction force resulted in compression at the sites that were under tension during protraction (Table IV), suggesting recovery of the suture. However, this recovery was partial and was

Table IV. Changes in sutural deformation after the protraction forces were removed

	Inferior RZMS		*Inferior LZMS*		*Superior RZMS*		*Superior LZMS*		*Right NFS*		*Left NFS*	
Pig number	*BAMP*	*RPHG*	*BAMP*	*RPHG*	*BAMP*	*RPHG*	*BAMP*	*RPHG*	*BAMP*	*RPHG*	*BAMP*	*RPHG*
53	−34	−1	−14	−15	−2	−4	−6	−9	9	35	6	10
54*	NA	NA	NA	NA	NA	NA	NA	NA	NA	NA	NA	NA
56	−43	−33	−15	−8	−3	−17	6	14	24	37	34	91
57	−26	−5	−3	−5	−29	−13	−6	1	−16	3	−18	7
58	−9	−18	−52	−35	−7	−14	−9	−5	−5	10	−5	17
59	−39	−25	−37	−27	−5	−9	−12	−4	9	19	5	14
61	−16	−32	−51	−21	−18	29	−78	−23	17	23	2	37
62	−18	−6	−46	−35	−14	−9	−33	−3	0	−2	6	19
63	−24	−30	−50	−41	−43	−40	−1	−15	−11	5	33	34
64	−8	−2	−3	−21	−3	−5	−12	−24	99	−83	−73	−86
65	0	0	−13	2	−20	−8	0	−27	−29	−14	NA	NA
66	−14	−13	−36	−12	−31	−20	−15	−36	−6	35	−10	16
67	−41	−5	−8	−1	−3	−5	−2	−1	−13	16	−4	10
Mean ± SD	−23 ± 14	−14 ± 13	−27 ± 20	−18 ± 14	−15 ± 14	−9 ± 16	−14 ± 22	−11 ± 14	7 ± 33	7 ± 32	−2 ± 28	15 ± 41
Median	−21	−10	−25	−18	−10	−9	−8	−7	−2	13	2	16

Values are standardized by 200 gf. Negative values indicate compression. Only animals with paired data from both BAMP and RPHG are reported.
NA, Not available; *SD*, standard deviation.
*No data from pig 54 because of error in file saving.

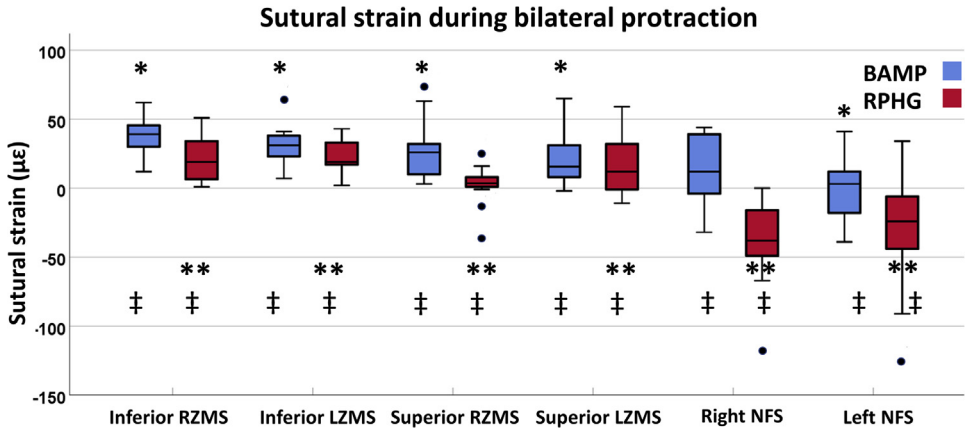

Fig 5. Box plot of the strain (per 200 gf) recorded by the strain gauges during the bilateral protraction experiments. The medians are represented as the *solid black horizontal lines*. The *box boundaries* correspond to the 25th and 75th percentile. *Whiskers* cover the 5th and the 95th percentile. *Black dots* correspond to the outliers. Significant differences: **P* <0.05 (within BAMP group); ***P* <0.002 (within RPHG group); ‡*P* <0.01 (BAMP vs RPHG).

approximately 55%-80% of the initial deformation caused by the protraction force.

DISCUSSION

In this study, we report on the deformation of the ZMS and NMS during 2 forms of maxillary protraction, including the tooth-supported RPHG and the bone-supported BAMP. Our study had several limitations, mainly because of the types of sensors used and the ex-vivo nature of the experiments. Two types of sensors were used, SG and DVRT. Although both have high resolution (approximately 1 με for the strain gages and approximately 1.5 μm for the DVRT), each is associated with some limitation. The DVRT sensing mechanism consists of 2 sliding elements, a core (rod) and cylinder (Fig 1). The sliding of the rod inside the cylinder measured the amount of separation of the suture. Because the DVRT is fixed to the bone using screws, the sensing mechanism is higher than the surface of the bone. As a result, the DVRT tends to underestimate

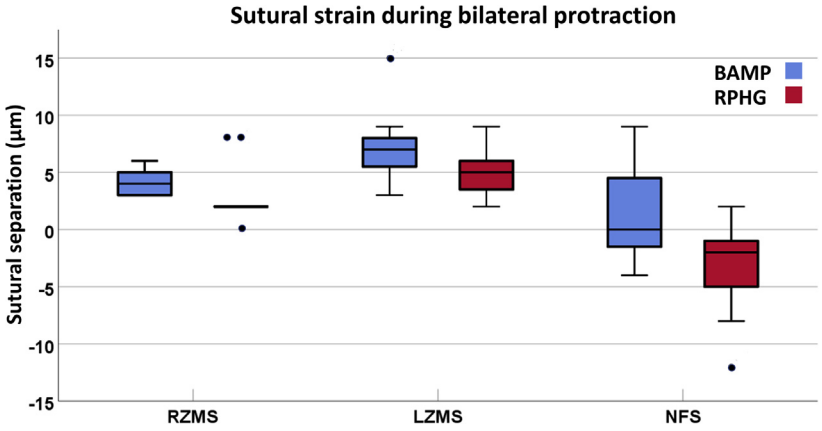

Fig 6. Descriptive summary of the linear separation of the ZMS and NFS recorded by the DVRTs during bilateral protraction. The medians are represented as the *solid black horizontal lines*. The *box boundaries* correspond to the 25th and 75th percentile. *Whiskers* cover the 5th and the 95th percentile. *Black dots* correspond to the outliers.

the movement that is not along the long axis of the sensor as the rod sliding is inhibited. In addition, some minor movement of the screw attachment cannot be ruled out. These factors might have contributed to the more significant variability in the DVRT results. However, the main advantage of the DVRTs is that they provide an absolute measurement of the deformation of the suture (in µm) rather than the ratio measurement (strain = change in length [△L]/original length [L]) reported by the SG. Thus, providing a more fixed reference number to sutural deformation during protraction. The SGs are in direct contact with the bone surface and thus provide a more accurate recording of the deformation of the suture. However, they cannot differentiate between anteroposterior (midface moving forward) and lateral (midface moving sideways) tension. Such limitation was addressed by conducting unilateral and bilateral protraction on each of the heads used. By observing the wave pattern during unilateral protraction, differentiating between anteroposterior and lateral tension was feasible. Sensors were placed in a standardized location in all the animals. In addition, because of the paired nature of the study (BAMP and RPHG on the same animals), any bias introduced by the discrepancy in the sensors' location would have been controlled.

Several limitations to this study were introduced by the ex-vivo nature of the experiment. The heads were obtained from a local abattoir; the age, gender, and breed were unknown. Obtaining the sample this way was a better alternative than using live animals for the sole purpose of collecting mechanical data. The lack of standardization in animals' age could have contributed to some of the variability in the results. This factor was controlled by selecting animals of comparable dental age. Another factor that could have added to the variability is the time lapse between animal killing and head freezing. Heads were stored at approximately 2°C after killing, obtained by our laboratory within 1-4 days and were immediately frozen at −20°C. Variation in time before freezing could have contributed to some of the variability. However, because both BAMP and RPHG were performed on the same heads, and the comparisons are paired, variability introduced by the above factors were controlled. Another limitation associated with the use of ex-vivo samples is the inability to study the biological impact of the mechanical loading of the sutures in the 2 groups. Although the effects of mechanical loading on bone formation at the sutures have long been known,[33,34] controversy still exists on the details of the relation between magnitude, pattern, and polarity of deformation and bone formation at the sutures. Our study reports only on the difference in mechanical loading of the sutures between RPHG and BAMP without assessing the biological impact of such difference. Although increased sutural separation observed in BAMP suggests an increase in bone formation, in-vivo studies are needed to support such claim.

The incremental addition of the 5 × 200 gf was intended to assess the relation between increased force magnitude and sutural deformation. Although sutural strain increased with the increased force magnitude, high variability was noticed. Some sites in some animals showed an equal increase in strain between each of the 200 gf increments, whereas others showed significant

variation with no apparent pattern. Variability was present among the same sites in different animals and different sites in the same animal. Thus, the relationship between increased force magnitude and sutural separation remains mostly unknown. As a result, the strain gauge data were reported as an average of the deformations recorded after each of the 200 gf elastics were applied in the unilateral protraction; and as an average of the deformations after each pair of the 200 gf elastics were applied in the bilateral protraction. Averaging strain values this way assumes comparable strain for each of the force intervals. Although this assumption carries some limitations, we believe it is the best way to present the data. It provides clinically relevant values while limiting the impact of extreme measures.

Bilateral protraction illustrated 2 significant differences between BAMP and RPHG, including the magnitude of sutural deformation and overall direction of maxillary protraction. The magnitude of sutural separation was higher in the BAMP group in most of the animals studied, which supports the notion that bypassing teeth and applying protraction force directly to the maxillary bone resulted in better force delivery and sutural separation.[35] Increased sutural separation is believed to result in more bone formation along the sutural edges.[28] This effect might explain some of the clinical findings of increased maxillary protraction in the BAMP group when compared with a combination of RPHG and rapid palatal expansion;[18,20] and could also explain the increase in mineral apposition in sutures undergoing BAMP compared with untreated controls.[24,25]

Another difference between the BAMP and RPHG is the overall pattern of protraction, which was clearly illustrated by the direction of deformation at the NFS. Most animals in the BAMP group recorded tension, whereas most of the animals in the RPHG displayed compression at the NFS. This finding together with the higher magnitude of tension at the inferior ZMS compared with the superior ZMS, suggest that BAMP resulted in a more horizontal (anteroposterior) protraction, although the direction of protraction in the RPHG is a combination of protraction and upward and backward rotation of the anterior maxilla. The effects of the direction of protraction force on the rotation of the maxilla in the RPHG have long been studied.[36] In an ex-vivo study on a human skull, Hata et al[37] reported drastic changes in the direction of the maxillary protraction when the protraction force was applied parallel, 5 mm and 10 mm above the occlusal plane. They further suggested that a protraction force that is 5 mm above the occlusal plane resulted in an almost pure anteroposterior movement of the maxilla. In contrast, a more recent clinical study Keles et al[38] suggested that a protraction force of 20 mm above the occlusal plane is needed for pure anteroposterior movement. Although the differences between these 2 studies can be explained by the difference in experimental methodology and design, it highlights the importance of understanding the protraction force vector on the overall movement of the maxilla. The force vector should pass through the center of rotation of the maxilla, estimated to be in the premolar root vicinity,[39] or in the critical ridge area below the zygomatic process of the maxilla to achieve a complete anteroposterior protraction.[40] Because the BAMP protraction vector is closer to the center of rotation of the maxilla suggested by Billiet,[40] a more horizontal protraction is feasible, which coincides with the clinical finding of Cevidanes[20] and Hino[18] that showed less rotation of the maxilla in the BAMP patients compared with RPHG patients.

Although anteroposterior protraction was the predominant pattern in BAMP, some animals showed a rotation pattern similar to that seen in the RPHG. A similar form of rotation was seen in some clinical studies.[18,20] This further highlights the importance of force direction on the overall protraction of the maxilla, especially in BAMP. The extraoral traction unit in the RPHG allows some adjustments in the angle of protraction. Such adjustment is minimal in case of BAMP because of the anatomical restrictions necessitated by the intraoral traction system. Thus, a thorough understanding of the relation between force direction and maxillary rotation in BAMP is needed.

Another factor that could have contributed to the rotations seen in BAMP is the variability in the ZMS itself. Studies in humans have shown significant variability in the shape of the facial surface of the suture.[41,42] Although some authors believe the variations in the ZMS are suggestive of the racial background of the subjects,[43-45] others showed that such variation exists regardless of the race.[42] Unfortunately, we did not investigate the shape of the ZMS in our sample. However, such variation, if present, can explain some of the inconsistency in protraction outcome. Additional research is needed to identify the prevalence of such variation and its effect on maxillary protraction, thus allowing treatments that are customizable to patients' anatomical differences.

Our results showed great variability in the magnitude of sutural deformation between individual animals. Some of this variability could have been introduced by variation in animals' age and by the level of ZMS maturity. Unfortunately, because of the way the heads were obtained, the age of the animals was unknown. However, animals were of comparable dental ages. Thus, some

of this variability might have been because of the differences in ZMS maturity. Human studies[46,47] proved that age alone is not an accurate predictor of the degree of ZMS maturation and the outcome of the maxillary protraction. Future studies should aim at observing the amount of sutural separation concerning the degree of sutural maturation, which will help provide an individualized treatment based on the patient's sutural age.

The magnitude of deformation of the ZMS was surprisingly small, especially in comparison with the amount of the maxillary protraction reported in clinical studies. For example, Hino et al[18] reported 3.7 mm of maxillary protraction in BAMP over approximately 1 year of treatment using a protraction force of 250 gf, which translates to approximately 10 μm of protraction per day and is more than double the 5.5 μm measured in this study using 1000 gf. Although such comparison is rudimentary and is further limited by lack of knowledge of the relation between sutural separation and bone formation at the suture, it suggests that the overall maxillary protraction seen during BAMP cannot be explained by ZMS separation alone. This finding suggests that the circummaxillary sutures, along with separation, transmit some of the protraction load to more distant sutures. Our finding of tension at the NFS in most of the BAMP heads supports such an assumption and suggests that the ZMS is not the sole target of BAMP. Histologically, the ZMS is the longest of the circummaxillary sutures and is heavily interdigitated.[33,48] Previous studies showed that applying protraction force to the maxilla resulted in the separation of several facial sutures.[33] Applying load to metal implants placed in the maxilla resulted in disarticulation of the ZMS and ZTS.[11] Similarly, Jackson et al[35] showed that protraction of the maxilla resulted in a comparable amount of separation of the ZMS and ZTS. This finding coincides well with ex-vivo literature that suggests comparable or greater separation at the ZTS compared with the ZMS.[37,49] In a clinical study, Nguyen et al[21] reported that the zygoma was protracted approximately 2 mm in BAMP patients. Determining how the facial sutures are loaded during BAMP is important because such loading might result in changes in facial morphology. Our study was focused on the vertical progression of the protraction load, and more posterior sutures such as the ZTS were not investigated. Future studies are needed to assess how BAMP loads various sutures of the head.

Results of the unilateral experiment clearly display that unilateral force application resulted in lateral movement of the midface toward the side opposite to force application. This finding coincides with a recent finite element analysis study that showed that asymmetrical force application results in asymmetrical protraction of the maxilla.[50] It also highlights the importance of symmetrical force application in case of bilateral protraction to avoid creating maxillary asymmetry. No clinical studies exist on unilateral protraction, which can be attributed to the fact that applying unilateral protraction force with the RPHG is limited because it will result in instability of the extraoral component. Such interference does not exist in BAMP. This suggests that BAMP can be used in a growing patient to address midfacial asymmetry. Further studies on this potential possibility are needed.

The effects of BAMP on the mandible are still poorly understood. Because of BAMP reliance on the mandible for anchorage, it is expected that BAMP will result in a posterior force on the mandible. In addition, movements of the mandible will have significant effects on BAMP force and the subsequent sutural deformation. The dynamic environment of mastication and muscle contraction is long known to contribute to sutural loading.[51] Recent studies suggest that BAMP has a chincup effect and might induce favorable rotation of the mandible.[22,32] We attempted to assess the relation between BAMP and mandibular movements by manually moving the mandible forward after all the protraction forces are applied. This method is rudimentary, lacked standardization, and does not replicate the dynamic environment of mastication. In addition, it was limited to a few millimeters because of the increased stiffness of the muscles of mastication postmortem. Thus, care should be exercised in interpreting our results and extending these findings to the dynamic environment in a living animal. Moving the mandible forward resulted in approximately 30% increase in strain at the ZMS and suggests that BAMP places posterior pressure of the mandible and that mandibular movements affect the sutural loading during protraction. The effects of such forces on the temporomandibular joint and bone formation at the sutures are still poorly understood and warrant further investigation.

Animals were monitored for 26 (SD 12) seconds after the protraction force was removed. Even with this relatively extended period of observation, some residual strain was present at the sutures. Although more strain was dissipated by the time the subsequent experiment was performed, some of this strain could have been carried to the following experiment affecting results. Comparing sutural deformation at each of the sites in the animals where BAMP was performed first (pigs 53-60) to those in which RPHG was performed first (pigs 61-67) showed relatively comparable results. This finding suggests that any error introduced by residual

strain was probably minimal and affected both groups equally. Nonetheless, this interesting finding suggests that sutures dissipate loads gradually. However, we did not measure the rate of load dissipation by the sutures as it was outside the scope of the current study. Future studies are needed to improve our understanding of this topic and its potential implications on skull loading during orthopedic treatment.

CONCLUSIONS

In this study, we report on the deformation of the ZMS and NFS during BAMP and RPHG treatment in ex-vivo pig heads. Within the limitations of this study, our results suggest the following:

1. Both BAMP and RPHG produce tension at the ZMS, with higher magnitude in BAMP.
2. There is a major difference between BAMP and RPHG at the NFS, with BAMP resulting in tension and RPHG compression of the suture.
3. BAMP produce a more anterior translation of the midface, whereas RPHG results in upward and backward rotation of the midface (counterclockwise in right-facing orientation).
4. More research is needed to explain why some BAMP subjects displayed a pattern of midface protraction similar to RPHG.
5. Unilateral application of BAMP may be useful in treatment of patients with maxillary asymmetry.

ACKNOWLEDGMENTS

The authors would like to thank Dr Sue Herring for providing some of the research instruments and supplies. The authors would also like to thank 2 anonymous reviewers for their comments and suggestions.

REFERENCES

1. Hardy DK, Cubas YP, Orellana MF. Prevalence of angle Class III malocclusion: a systematic review and meta-analysis. Open J Epidemiol 2012;2:75-82.
2. Guyer EC, Ellis EE 3rd, McNamara JA Jr, Behrents RG. Components of Class III malocclusion in juveniles and adolescents. Angle Orthod 1986;56:7-30.
3. Hägg U, Tse A, Bendeus M, Rabie AB. Long-term follow-up of early treatment with reverse headgear. Eur J Orthod 2003;25:95-102.
4. Nanda R, Hickory W. Zygomaticomaxillary suture adaptations incident to anteriorly-directed forces in rhesus monkeys. Angle Orthod 1984;54:199-210.
5. Delaire J. Maxillary development revisited: relevance to the orthopaedic treatment of Class III malocclusions. Eur J Orthod 1997;19:289-311.
6. Nartallo-Turley PE, Turley PK. Cephalometric effects of combined palatal expansion and facemask therapy on Class III malocclusion. Angle Orthod 1998;68:217-24.
7. Williams MD, Sarver DM, Sadowsky PL, Bradley E. Combined rapid maxillary expansion and protraction facemask in the treatment of Class III malocclusions in growing children: a prospective long-term study. Semin Orthod 1997;3:265-74.
8. Kapust AJ, Sinclair PM, Turley PK. Cephalometric effects of face mask/expansion therapy in Class III children: a comparison of three age groups. Am J Orthod Dentofacial Orthop 1998;113:204-12.
9. Baccetti T, McGill JS, Franchi L, McNamara JA Jr, Tollaro I. Skeletal effects of early treatment of Class III malocclusion with maxillary expansion and face-mask therapy. Am J Orthod Dentofacial Orthop 1998;113:333-43.
10. Kokich VG, Shapiro PA, Oswald R, Koskinen-Moffett L, Clarren SK. Ankylosed teeth as abutments for maxillary protraction: a case report. Am J Orthod 1985;88:303-7.
11. Smalley WM, Shapiro PA, Hohl TH, Kokich VG, Brånemark PI. Osseointegrated titanium implants for maxillofacial protraction in monkeys. Am J Orthod Dentofacial Orthop 1988;94:285-95.
12. Esenlik E, Ağlarcı C, Albayrak GE, Fındık Y. Maxillary protraction using skeletal anchorage and intermaxillary elastics in skeletal Class III patients. Korean J Orthod 2015;45:95-101.
13. Feng X, Li J, Li Y, Zhao Z, Zhao S, Wang J. Effectiveness of TAD-anchored maxillary protraction in late mixed dentition. Angle Orthod 2012;82:1107-14.
14. Ge YS, Liu J, Chen L, Han JL, Guo X. Dentofacial effects of two facemask therapies for maxillary protraction. Angle Orthod 2012;82:1083-91.
15. Cha BK, Choi DS, Ngan P, Jost-Brinkmann PG, Kim SM, Jang IS. Maxillary protraction with miniplates providing skeletal anchorage in a growing Class III patient. Am J Orthod Dentofacial Orthop 2011;139:99-112.
16. Kircelli BH, Pektaş ZO, Uçkan S. Orthopedic protraction with skeletal anchorage in a patient with maxillary hypoplasia and hypodontia. Angle Orthod 2006;76:156-63.
17. De Clerck H, Cevidanes L, Baccetti T. Dentofacial effects of bone-anchored maxillary protraction: a controlled study of consecutively treated Class III patients. Am J Orthod Dentofacial Orthop 2010;138:577-81.
18. Hino CT, Cevidanes LH, Nguyen TT, De Clerck HJ, Franchi L, McNamara JA Jr. Three-dimensional analysis of maxillary changes associated with facemask and rapid maxillary expansion compared with bone anchored maxillary protraction. Am J Orthod Dentofacial Orthop 2013;144:705-14.
19. Baccetti T, De Clerck HJ, Cevidanes LH, Franchi L. Morphometric analysis of treatment effects of bone-anchored maxillary protraction in growing Class III patients. Eur J Orthod 2011;33:121-5.
20. Cevidanes L, Baccetti T, Franchi L, McNamara JA Jr, De Clerck H. Comparison of two protocols for maxillary protraction: bone anchors versus face mask with rapid maxillary expansion. Angle Orthod 2010;80:799-806.
21. Nguyen T, Cevidanes L, Cornelis MA, Heymann G, de Paula LK, De Clerck H. Three-dimensional assessment of maxillary changes associated with bone anchored maxillary protraction. Am J Orthod Dentofacial Orthop 2011;140:790-8.
22. Nguyen T, Cevidanes L, Paniagua B, Zhu H, Koerich L, De Clerck H. Use of shape correspondence analysis to quantify skeletal changes associated with bone-anchored Class III correction. Angle Orthod 2014;84:329-36.
23. Nguyen T, De Clerck H, Wilson M, Golden B. Effect of Class III bone anchor treatment on airway. Angle Orthod 2015;85:591-6.
24. Ito Y, Kawamoto T, Moriyama K. The orthopaedic effects of bone-anchored maxillary protraction in a beagle model. Eur J Orthod 2014;36:632-40.

25. Al Dayeh A. Sutural loading during bone-anchored maxillary protraction. In: Kapila SD, Vig KW, Huang GJ, De Koster KY, editors. Anecdote, Expertise and Evidence: Applying New Knowledge to Everyday Orthodontics. Ann Arbor, MI: Department of Orthodontics and Pediatric Dentistry, School of Dentistry, University of Michigan; 2017. p. 41-67.
26. Mao JJ, Wang X, Kopher RA. Biomechanics of craniofacial sutures: orthopedic implications. Angle Orthod 2003;73:128-35.
27. Liu SS-Y, Kyung HM, Buschang PH. Continuous forces are more effective than intermittent forces in expanding sutures. Eur J Orthod 2010;32:371-80.
28. Liu SS-Y, Opperman LA, Kyung HM, Buschang PH. Is there an optimal force level for sutural expansion? Am J Orthod Dentofacial Orthop 2011;139:446-55.
29. Oberheim MC, Mao JJ. Bone strain patterns of the zygomatic complex in response to simulated orthopedic forces. J Dent Res 2002; 81:608-12.
30. Mao JJ, Wang X, Mooney MP, Kopher RA, Nudera JA. Strain induced osteogenesis of the craniofacial suture upon controlled delivery of low-frequency cyclic forces. Front Biosci 2003;8: a10-7.
31. Chen L, Chen R, Yang Y, Ji G, Shen G. The effects of maxillary protraction and its long-term stability—a clinical trial in Chinese adolescents. Eur J Orthod 2012;34:88-95.
32. De Clerck H, Nguyen T, de Paula LK, Cevidanes L. Three-dimensional assessment of mandibular and glenoid fossa changes after bone-anchored Class III intermaxillary traction. Am J Orthod Dentofacial Orthop 2012;142:25-31.
33. Kambara T. Dentofacial changes produced by extraoral forward force in the Macaca irus. Am J Orthod 1977;71:249-77.
34. Burstone CJ, Shafer WG. Sutural expansion by controlled mechanical stress in the rat. J Dent Res 1959;38:534-40.
35. Jackson GW, Kokich VG, Shapiro PA. Experimental and postexperimental response to anteriorly directed extraoral force in young Macaca nemestrina. Am J Orthod 1979;75:318-33.
36. Yepes E, Quintero P, Rueda ZV, Pedroza A. Optimal force for maxillary protraction facemask therapy in the early treatment of Class III malocclusion. Eur J Orthod 2014;36:586-94.
37. Hata S, Itoh T, Nakagawa M, Kamogashira K, Ichikawa K, Matsumoto M, et al. Biomechanical effects of maxillary protraction on the craniofacial complex. Am J Orthod Dentofacial Orthop 1987;91:305-11.
38. Keles A, Tokmak EC, Erverdi N, Nanda R. Effect of varying the force direction on maxillary orthopedic protraction. Angle Orthod 2002; 72:387-96.
39. Nanda R. Biomechanical and clinical considerations of a modified protraction headgear. Am J Orthod Dentofacial Orthop 1980;78: 125-39.
40. Billiet T, de Pauw G, Dermaut L. Location of the centre of resistance of the upper dentition and the nasomaxillary complex. An experimental study. Eur J Orthod 2001;23:263-73.
41. Hefner JT. Cranial nonmetric variation and estimating ancestry. J Forensic Sci 2009;54:985-95.
42. L'Abbé EN, Van Rooyen C, Nawrocki SP, Becker PJ. An evaluation of non-metric cranial traits used to estimate ancestry in a South African sample. Forensic Sci Int 2011;209:195.e1-7.
43. Iscan MY, Steyn M. The human skeleton in forensic medicine. 3rd ed. Charles C Thomas Publisher Limited; 2013.
44. Sholts SB, Wärmländer SK. Zygomaticomaxillary suture shape analyzed with digital morphometrics: reassessing patterns of variation in American Indian and European populations. Forensic Sci Int 2012;217:234.e1-6.
45. Oettlé AC, Demeter FP, L'abbé EN. Ancestral variations in the shape and size of the zygoma. Anat Rec (Hoboken) 2017;300: 196-208.
46. Angelieri F, Franchi L, Cevidanes LHS, Hino CT, Nguyen T, McNamara JA Jr. Zygomaticomaxillary suture maturation: a predictor of maxillary protraction? Part I - a classification method. Orthod Craniofac Res 2017;20:85-94.
47. Angelieri F, Ruellas AC, Yatabe MS, Cevidanes LHS, Franchi L, Toyama-Hino C, et al. Zygomaticomaxillary suture maturation: part II-the influence of sutural maturation on the response to maxillary protraction. Orthod Craniofac Res 2017;20:152-63.
48. Miroue M, Rosenberg L. The human facial sutures: a morphologic and histologic study of age changes from 20 to 95 years: [Thesis]. Seattle, WA: University of Washington; 1975.
49. Lee KG, Ryu YK, Park YC, Rudolph DJ. A study of holographic interferometry on the initial reaction of maxillofacial complex during protraction. Am J Orthod Dentofacial Orthop 1997;111:623-32.
50. Chen Z, Pan X, Zhao N, Chen Z, Shen G. Asymmetric maxillary protraction for unilateral cleft lip and palate patients using finite element analysis. J Craniofac Surg 2015;26:388-92.
51. Herring SW, Ochareon P. Bone—special problems of the craniofacial region. Orthod Craniofac Res 2005;8:174-82.